

Noninvasive Measurement of Protein Aggregation by Mutant Huntingtin Fragments or α -Synuclein in the Lens*

Received for publication, November 27, 2007, and in revised form, December 24, 2007. Published, JBC Papers in Press, December 31, 2007, DOI 10.1074/jbc.M709678200

Paul J. Muchowski^{†1}, Richard Ramsden[‡], QuangVu Nguyen[‡], Ernest E. Arnett[§], Teri M. Greiling[§], Susan K. Anderson[§], and John I. Clark^{§12}

From the Departments of [†]Pharmacology, [§]Biological Structure, and [¶]Ophthalmology, University of Washington, Seattle, Washington 98195

Many diverse human diseases are associated with protein aggregation in ordered fibrillar structures called amyloid. Amyloid formation may mediate aberrant protein interactions that culminate in neurodegeneration in Alzheimer, Huntington, and Parkinson diseases and in prion encephalopathies. Studies of protein aggregation in the brain are hampered by limitations in imaging techniques and often require invasive methods that can only be performed post-mortem. Here we describe transgenic mice in which aggregation-prone proteins that cause Huntington and Parkinson disease are expressed in the ocular lens. Expression of a mutant huntingtin fragment or α -synuclein in the lens leads to protein aggregation and cataract formation, which can be monitored in real time by noninvasive, highly sensitive optical techniques. Expression of a mutant huntingtin fragment in mice lacking the major lens chaperone, α B-crystallin, markedly accelerated the onset and severity of aggregation, demonstrating that the endogenous chaperone activity of α B-crystallin suppresses aggregation *in vivo*. These novel mouse models will facilitate the characterization of protein aggregation *in vivo* and are being used in efficient and economical screens for chemical and genetic modifiers of disease-relevant protein aggregation.

A critical obstacle for identifying potential therapeutic compounds to treat neurodegenerative diseases, such as Alzheimer disease, Parkinson disease (PD),³ and Huntington

disease (HD), is the lack of cost-effective animal models for rapid tests of drug bioavailability, pharmacokinetics, and efficacy. HD is an autosomal dominant inherited disorder characterized by involuntary movements, personality changes, and dementia. It is caused by an expansion of a CAG repeat in the first exon of the gene *IT-15* (1). A neuropathological hallmark of HD is intranuclear and cytoplasmic inclusion bodies that contain a mutant form of huntingtin (htt), the protein encoded by *IT-15* (2). Cytoplasmic inclusion bodies (called Lewy bodies) are also a prominent feature of PD, a neurodegenerative disorder characterized by muscle rigidity, bradykinesia, resting tremor, and postural instability (3). Lewy bodies are composed primarily of the protein α -synuclein. Three point mutations in the α -synuclein gene, as well as triplication of the wild-type locus, cause early onset, inherited forms of PD (4). Mutant htt fragments and α -synuclein aggregate into ordered fibrillar structures with properties of amyloid (5, 6).

Although amyloid or its formation is closely associated with the pathogenesis of many neurodegenerative diseases, it has been a technical challenge to characterize protein aggregation in the brain noninvasively. The ocular lens is a unique immune-privileged tissue derived from neural ectoderm that contains the only transparent cells found in the entire body. Disruption of normal protein interactions in the lens leads to protein aggregation and cataract formation, which can be monitored easily and repetitively in living animals by highly sensitive noninvasive methods. The lens is an optically accessible tissue that would be ideal for the study of disease-relevant protein aggregation. We hypothesized that expression of disease-causing, aggregation-prone proteins in the lens would lead to cataract formation that could be measured in living mice.

EXPERIMENTAL PROCEDURES

Generation of Transgenic Mice—To generate mice expressing mutant htt fragments with 25Q, 46Q, 72Q, and 97Q, the first exon of the *IT-15* gene with DNA sequence encoding selected polyglutamine (polyQ) repeat lengths (25Q, 46Q, 72Q, or 97Q) fused to enhanced green fluorescent protein (GFP) at the carboxyl terminus was excised from parental vectors (7) with Bsp120I, filled in with Klenow, and gel-purified. Before ligation, a construct containing the murine α A-crystallin vector (8) was digested with BamHI, filled in with Klenow, and digested with HpaI. The digested vector was treated with shrimp alkaline phosphatase, gel-purified, and ligated to htt fragments. All constructs were confirmed by direct sequencing.

* This study was supported by grants from the Hereditary Disease Foundation under the auspices of the "Cure Huntington's Disease Initiative," the HighQ Foundation, and the Nathan Shock Center of Excellence in the Basic Biology of Aging and from the Royalty Research Fund at the University of Washington (to P. J. M.) and by Grant EY04552 from the National Eye Institute (to J. I. C.) and a grant from the Royalty Research Fund from the University of Washington (to P. J. M.). The costs of publication of this article were defrayed in part by the payment of page charges. This article must therefore be hereby marked "advertisement" in accordance with 18 U.S.C. Section 1734 solely to indicate this fact.

¹ To whom correspondence should be addressed. Gladstone Institute of Neurological Disease, Dept. of Biochemistry and Biophysics, and Dept. of Neurology, University of California, San Francisco, California, 94158. Tel.: 415-734-2515; Fax: 415-355-0824; E-mail: pmuchowski@gladstone.ucsf.edu.

² Supported by the U. S. National Eye Institute.

³ The abbreviations used are: PD, Parkinson disease; HD, Huntington disease; BSA, bovine serum albumin; GFP, green fluorescent protein; EGFP, enhanced GFP; htt, huntingtin; PBS, phosphate-buffered saline; polyQ, polyglutamine; QLS, quasielastic laser light scattering spectroscopy; α -Syn-WT, wild-type α -synuclein; GAPDH, glyceraldehyde-3-phosphate dehydrogenase.

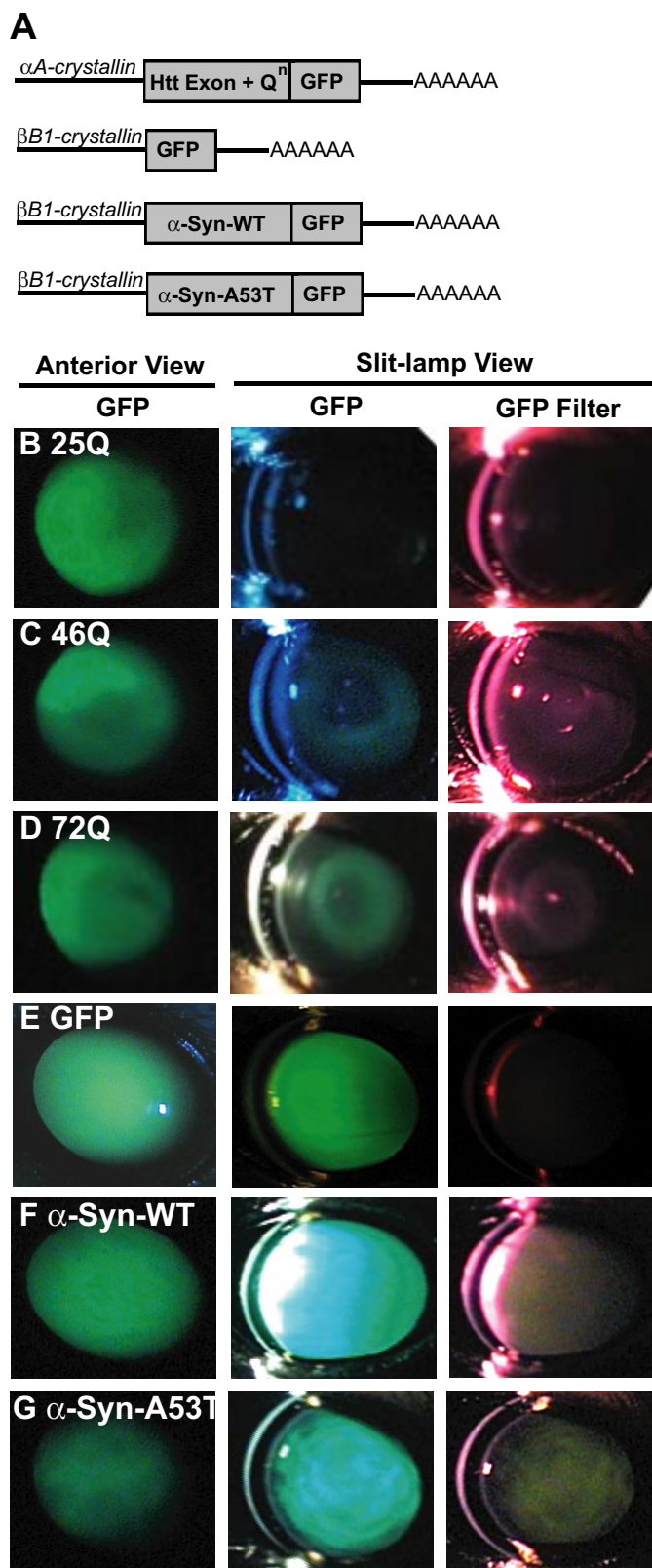


FIGURE 1. Targeted expression of mutant htt fragments or α -synuclein to the ocular lens causes cataract formation. A, schematic diagram of targeting constructs used to generate transgenic mice. B–G, digital images of transgenic mice expressing 25Q, 46Q, or 72Q (B–D), GFP, α -Syn-WT, or α -Syn-A53T (E–G). In the first column, images of the anterior view of lenses were captured under conditions of GFP excitation and emission. In the second column, images were captured under conditions of GFP excitation and emission using a slit-lamp biomicroscope that shows an optical section through the lens. In

the third column, images were captured with a slit-lamp biomicroscope using a filter that blocks light emitted by GFP. The lenses of 46Q and 72Q mice contain a shell of opacity that corresponds to a supranuclear cataract, whereas the 25Q animal has no opacity/opacity. Likewise, lenses of α -Syn-WT and α -Syn-A53T mice contain a large opacity, whereas the mouse that expresses GFP alone has no opacity/opacity.

Transgenes were excised from the vector with AatII and NgoMIV and gel-purified. DNA was precipitated with isopropyl alcohol and resuspended in a buffer containing 10 mM Tris, pH 8.0. Transgenes were dialyzed for 2 h against 10 mM Tris, 0.1 mM EDTA (pH 8.0) prepared from embryo-tested water (Sigma) on a 0.1- μ m VCWP filter (Millipore). The dialyzed transgenes were used for pronuclear microinjection into B6C3 mouse embryos (75% C57BL/6 and 25% C3H) at the animal facilities of the Department of Comparative Medicine at the University of Washington. Founder mice were identified by DNA amplification with *Taq* polymerase (Invitrogen) from tail biopsy material with primers directed against enhanced GFP. Positive mice were mated with C57BL/6 mice; the offspring were similarly identified.

To generate GFP, wild-type α -synuclein (α -Syn-WT), and α -Syn-A53T mice, a vector containing the chicken β B1-crystallin promoter (9), was digested with XbaI and XhoI, treated with shrimp alkaline phosphatase, and gel-purified before DNA ligations. DNA sequences encoding α -Syn-WT and α -Syn-A53T fused to GFP were excised from p426GPD vectors (10) with SpeI and XhoI and were gel-purified. A DNA sequence encoding GFP alone was amplified from p426GPD with primers that create XbaI (5') and XhoI (3') overhangs and was gel-purified. After ligation reactions, transgenes were excised with KpnI and BglI, gel-purified, and used for pronuclear microinjections as described above.

Slit-lamp Ophthalmoscopy—3–12-week-old animals were analyzed by digital imaging coupled to a slit-lamp biomicroscope as described previously (11). The opacity from the heterogeneous protein aggregates in lens cells can be observed routinely using a slit lamp in the absence of filters. The incident light for slit-lamp observations included the excitation wavelengths for EGFP absorption and emission filters (Chroma Technology Corp., Rockingham, VT). Using the filters, it was possible to distinguish between the fluorescence from the expression of GFP proteins and light scattering from protein aggregates having a broad range of dimensions. An excitation filter allowed a narrow range of incident wavelengths (λ 465–498 nm) to excite EGFP (excitation max: λ 488 nm) expressed in the lens. An emission filter transmitted wavelengths (λ 515–560 nm) originating from EGFP fluorescence (emission max: λ 507 nm). Lastly, a barrier filter for EGFP emission (λ 475–560 nm) was used to block EGFP emission and observe the scattering from protein aggregates.

Quasielastic Laser Light Scattering Spectroscopy (QLS)—Unanesthetized mice were gently restrained by hand while a low power beam of an 0.3-milliwatt laser ($\lambda = 780$ nm) was focused in the lens. The intensity fluctuations of the scattered light were recorded for 1 s, and the autocorrelation function for the intensity fluctuations was plotted.

Confocal Microscopy of Lens Sections—Eyes were removed from euthanized mice, embedded in OCT, and frozen in a

the third column, images were captured with a slit-lamp biomicroscope using a filter that blocks light emitted by GFP. The lenses of 46Q and 72Q mice contain a shell of opacity that corresponds to a supranuclear cataract, whereas the 25Q animal has no opacity/opacity. Likewise, lenses of α -Syn-WT and α -Syn-A53T mice contain a large opacity, whereas the mouse that expresses GFP alone has no opacity/opacity.

Aggregation of Mutant Huntingtin and α -Synuclein in the Lens

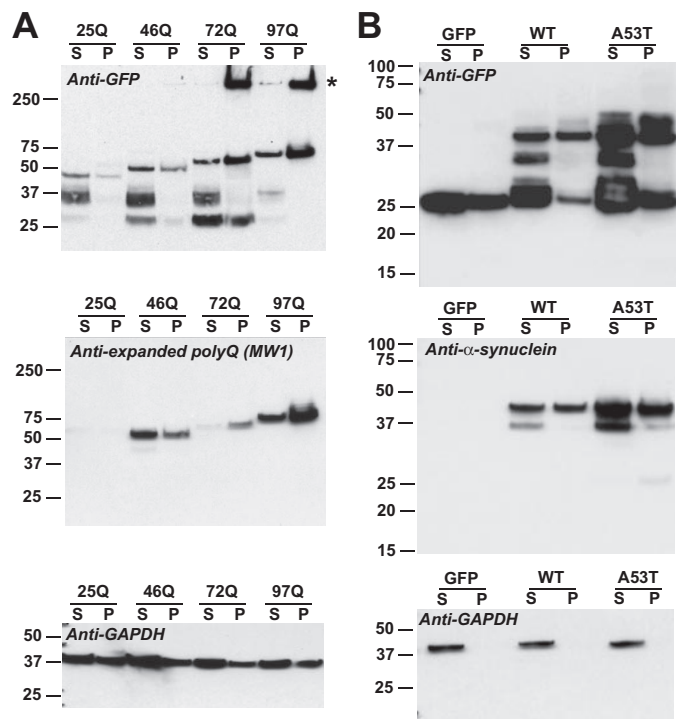


FIGURE 2. Targeted expression of mutant htt fragments or α -synuclein to the ocular lens. *A*, immunoblot analyses of lens-cell lysates (S = soluble, P = pellet) from transgenic animals that express mutant huntingtin fragments with 25Q, 46Q, 72Q, or 97Q, probed with antibodies against GFP, expanded polyQ protein (MW1), or GAPDH. *B*, immunoblot analyses of lens-cell lysates from transgenic animals expressing GFP, α -Syn-WT (WT), or α -Syn-A53T (A53T) probed with antibodies against GFP, α -synuclein, or GAPDH.

dry ice, 95% ethanol bath. Sections (10–20- μ m) were cut on a cryostat, picked up on Superfrost Plus slides (VWR International), air-dried overnight, and stored at -80°C . Slides were fixed for 10 min with -20°C acetone or for 20 min with 4% paraformaldehyde in 0.1 M phosphate buffer, pH 7.4. These fixatives gave similar results. Slides were washed three times in phosphate-buffered saline (PBS), 1% bovine serum albumin (BSA) between steps. Sections were labeled with propidium iodide (1 $\mu\text{g}/\text{ml}$ in PBS, 1% BSA) for 30 min; with wheat germ agglutinin conjugated to tetramethylrhodamine isothio-cyanate-dextran (Vector Laboratories) in PBS, 1% BSA for 60 min; with Nile Red (0.1–0.5 $\mu\text{g}/\text{ml}$ in PBS) for 10 min; or with rabbit polyclonal antibody against β -catenin (1:500 in PBS, 1% BSA; Sigma) for 60 min. The latter was visualized with Alexa Fluor 568 goat anti-rabbit IgG (Molecular Probes). Slides were coverslipped with VECTASHIELD mounting medium (Vector Laboratories) and imaged with a Bio-Rad MRC 600 laser scanning confocal microscope and Comos software or with a Bio-Rad Radiance 2000 MP confocal microscope and LaserSharp 2000 software. The images were analyzed with Adobe PhotoShop.

RESULTS

Expression of Mutant htt Fragments or α -Synuclein in the Lens Causes Cataract Formation—We generated transgenic mice that express htt exon 1 with a polyQ repeat in the normal (25Q) and disease-causing (46Q, 72Q, 97Q) range fused at the carboxyl terminus to GFP under the control of the lens-specific

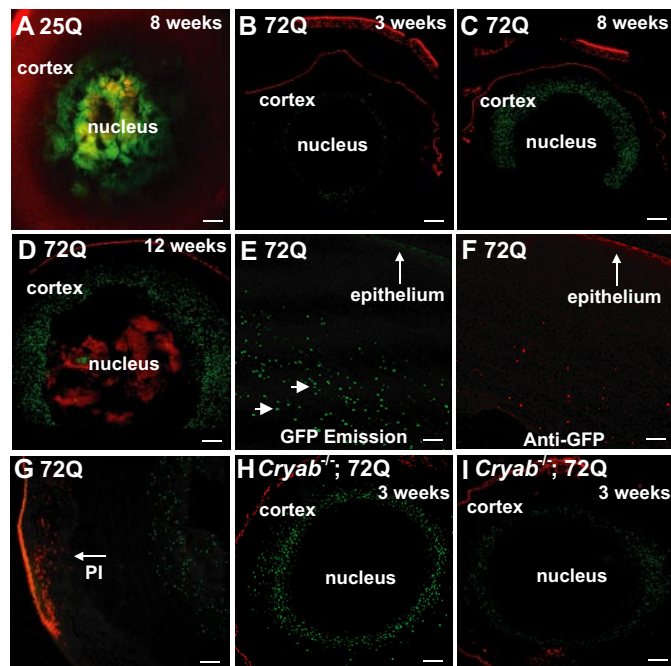


FIGURE 3. Targeted expression of a mutant htt fragment to the ocular lens results in the progressive formation of inclusion bodies. *A–D*, montages of digital images collected using a $\times 10$ objective from lens sections derived from a 25Q mouse aged 8 weeks (*A*) and from 72Q mice aged 3, 8, and 12 weeks (*B–D*). *A*, fiber cell membranes labeled with wheat germ agglutinin are shown in red. Between 3 and 12 weeks, the thickness of the shell of inclusion bodies in the lenses of 72Q mice increased >15 -fold. *E* and *F*, lens section from a 72Q transgenic mouse examined with a $\times 20$ objective showing GFP fluorescence (green) (*E*) or labeling with an anti-GFP antibody (red) (*F*). The average diameter of inclusion bodies increased in cells located more centrally in the lens (arrowheads), and not all inclusions were labeled anti-GFP antibody. *G*, 72Q inclusion bodies (green) form in the deep cortical region of the lens that is composed of anucleated cells. Nucleated cells in lens epithelial cells and differentiating fiber cells are labeled in red with propidium iodide (PI). *H* and *I*, the thickness of the shell of inclusion bodies in the lenses of 72Q mice lacking α B-crystallin (*Cryab*^{-/-};72Q) aged 3 weeks is approximately the same as in *Cryab*^{+/-};72Q mice aged 12 weeks (for *H* and *I*, representative images from two independent mice are shown). *A–D*, *H*, and *I*, the cortex and nucleus refer to anatomical designations for the central and peripheral regions of the lens, respectively. *B–I*, GFP fluorescence is shown in green, and staining for nuclei with propidium iodide is shown in red. Scale bar = 50 μm .

α A-crystallin promoter (8) (Fig. 1*A*). We also generated transgenic mice that express GFP alone or wild-type (α -Syn-WT) or mutant (α -Syn-A53T) α -synuclein fused to GFP at the carboxyl terminus (Fig. 1*A*). The latter mice were generated with the lens-specific β B1-crystallin promoter (9) due to the difficulty in obtaining founder lines with high expression levels using the α A-crystallin promoter (data not shown).

The lenses of young (6–12-week-old) transgenic mice were evaluated for GFP expression and cataract formation by digital imaging with a slit-lamp biomicroscope (11) (Fig. 1, *B–G*). In 25Q mice, GFP fluorescence was diffusely distributed throughout the lens, and no opacity was observed in the slit-lamp views (Fig. 1*B*). In 46Q and 72Q mice, however, GFP fluorescence was localized in a discrete shell surrounding the center of the lens (defined anatomically as the nucleus) (Fig. 1, *C* and *D*). When GFP fluorescence in the 46Q and 72Q lenses was blocked with a GFP emission filter, a shell of light scattering in the supranuclear or deep cortical region of the lens was revealed (Fig. 1, *C* and *D*). Supranu-

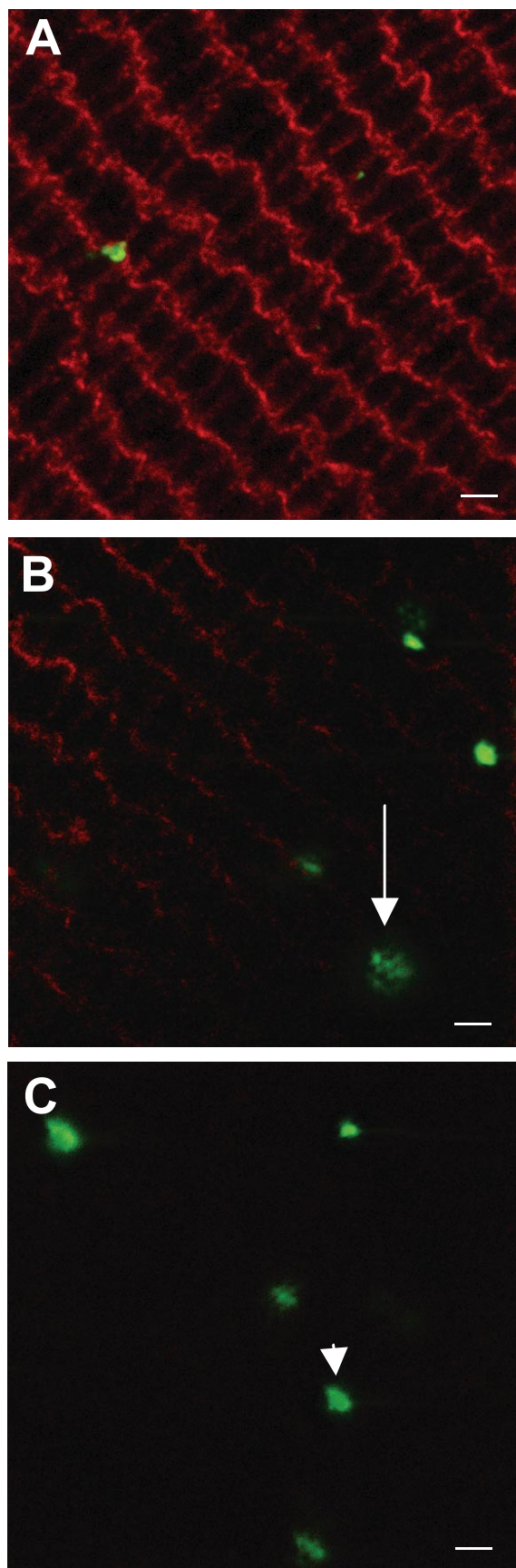


FIGURE 4. A mutant htt fragment forms large (1–5 μ m) intracellular inclusion bodies in lens cells. Z projections of five consecutive slices in different layers of a 72Q lens. *A*, in the lens cortex, inclusion bodies are small (diameter,

clear opacities were observed in seven independently generated 72Q transgenic mouse lines (data not shown). Supranuclear opacities, although quite rare in the normal human population, may exist in the lenses of Alzheimer disease patients and serve as a biomarker for disease progression (12).

In mice expressing GFP or α -Syn-WT/ α -Syn-A53T fused to GFP, a strong fluorescent signal was observed in anterior views of the lenses (Fig. 1, *E–G*). In slit-lamp images, GFP fluorescence was in the lens epithelium and distributed throughout the fiber cells. Images captured when GFP emission was blocked with a filter revealed a dense lenticular opacity only in mice expressing α -Syn-WT or α -Syn-A53T (Fig. 1, *F* and *G*). Mice expressing GFP alone had no signs of opacity (Fig. 1*E*).

Next, we analyzed immunoblots of protein lysates from the lens with antibodies that recognize expanded polyQ sequences or GFP. The polyQ-expressing mice (25Q–97Q) had similar levels of transgene expression (Fig. 2*A*). Importantly, as in transgenic mouse models of HD (13), SDS-insoluble aggregates that could not migrate into the gel matrix were observed in the pellet fraction of cellular lysates from 46Q, 72Q, and 97Q mice but not from 25Q mice (Fig. 2*A*). Thus, SDS-insoluble aggregates form in a polyQ length-dependent manner when htt exon 1 is expressed as a transgene in lens cells. Probing of immunoblots with anti-GFP antibody revealed GFP degradation products in lens lysates from 25Q–97Q mice. Expression of the htt exon 1 transgene with all polyQ lengths tested caused a significant fraction of GAPDH (the loading control in the gel) to shift to the pellet fraction (Fig. 2*A*). Since htt interacts directly with GAPDH *in vitro* (14), these results suggest that expression of htt exon 1 in lens cells mediates a redistribution of GAPDH to a particulate fraction by a physical interaction.

Immunoblot analysis of protein lysates from the lenses with antibodies that recognize α -synuclein or GFP showed similar levels of transgene expression in GFP, α -Syn-WT, and α -Syn-A53T mice (Fig. 2*B*). As in 25Q–97Q mice, probing of immunoblots with an anti-GFP antibody showed some protein degradation in lens lysates from α -Syn-WT and α -Syn-A53T mice.

Expression of a Mutant htt Fragment in the Lens Causes Supranuclear Inclusion Bodies—Lenses from 25Q and 72Q mice were analyzed in cryostat sections by confocal microscopy (Fig. 3). Consistent with the slit-lamp analyses (Fig. 1*B*), diffuse GFP fluorescence was observed in the lens nucleus in 25Q mice (Fig. 3*A*). However, sections from 72Q mice contained numerous distinct foci of GFP fluorescence resembling inclusion bodies that formed in a concentric shell around the nucleus; the thickness of the shell increased from \sim 10 to 200 μ m between 3 and 12 weeks of age (Fig. 3, *B–D*), which coincided with an increase in opacification observed by slit-lamp analyses (data not shown).

\sim 1 μ m) and appear to be associated with the fiber cell membrane. *B*, on the border of the lens cortex and nucleus, smaller particles are observed (arrow) that may coalesce into larger inclusion bodies. *C*, in the lens nucleus, only large inclusion bodies (\sim 7 μ m) are observed. Green indicates GFP fluorescence, and red indicates the lens fiber cell membrane (labeled with an antibody to β -catenin). Scale bar = 7 μ m.

Aggregation of Mutant Huntingtin and α -Synuclein in the Lens

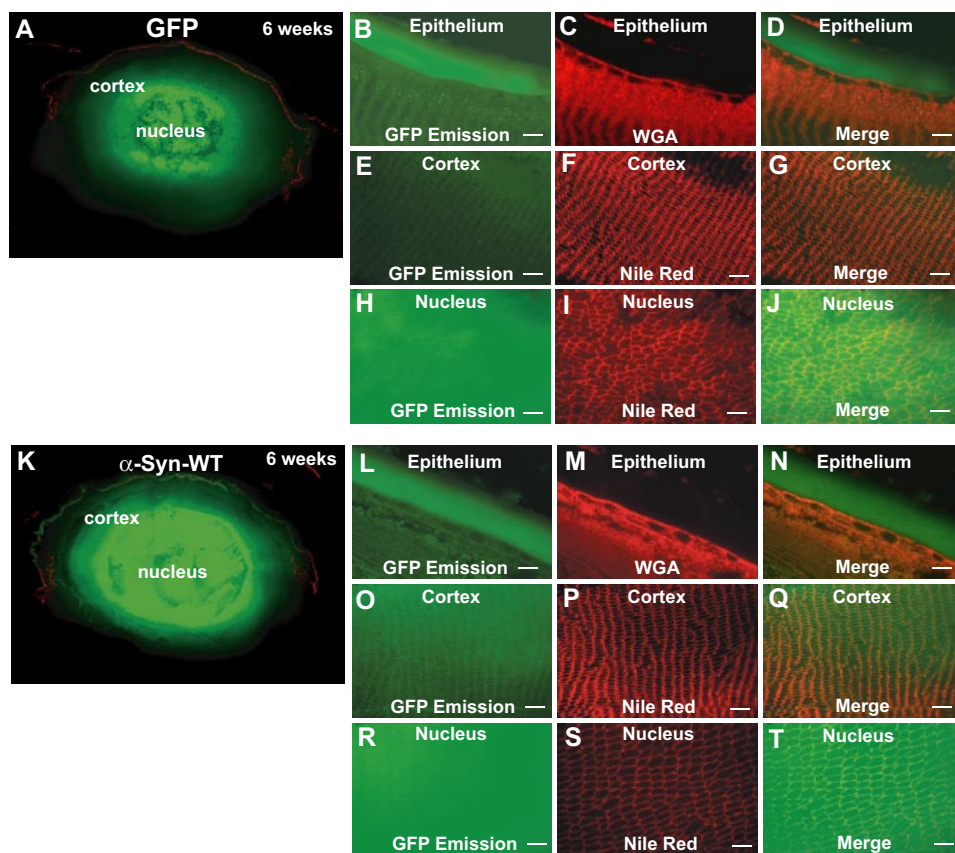


FIGURE 5. Targeted expression of α -synuclein to the ocular lens results in membrane and cytoplasmic localization. A and K, montages of digital $\times 10$ images of lens sections from GFP or α -Syn-WT mice aged 6 weeks. GFP fluorescence is shown in green, and staining for nuclei with propidium iodide is shown in red. B–J and L–T, montages of $\times 60$ digital images of lens sections showing the anterior epithelium (B–D, L–N), the cortex (E–G, O–Q), and the nucleus (H–J, R–T). GFP fluorescence is labeled in green. Red indicates the lens fiber cell membranes as labeled by Nile red (F, I, P, and S) or wheat germ agglutinin (WGA, C and M). Yellow indicates co-localization of fluorescence in merged images (D, G, J, N, Q, and T). Scale bar = 20 μ m.

The shell of inclusion bodies in 72Q mice was limited to a small region between the lens nucleus and cortex, also known as the supranuclear region or deep cortical region (Fig. 3, E–G). This region is composed of differentiated fiber cells that have lost all cellular organelles, including the nucleus. The molecular basis for the regional specificity of inclusion body formation in the lens is unclear but may be attributed to differences in the local concentration of chaperones and protein degradation machinery found in different regions of the lens. Some of the inclusion bodies could be labeled with an antibody against GFP (compare Fig. 3E with Fig. 3F). Although lens epithelial cells and differentiating fiber cells contain active proteasomes and ubiquitination machinery, the inclusion bodies in 72Q mice were deep to the layer of fiber cell differentiation (Fig. 3G) and did not react with ubiquitin antibodies (data not shown). The fluorescent foci were 3–5 μ m in diameter (Fig. 4), similar in size to inclusion bodies found in the brains of HD patients (2) and animal models (13). The average diameters of the inclusion bodies increased in older cells located closer to the center of the lens, and inclusion bodies were typically observed adjacent to lens fiber cell membranes (Fig. 4, A–C).

α B-Crystallin Suppresses Inclusion Body Formation in 72Q Mice—Since nearly 30% of protein in the lens is composed of a chaperone called α -crystallin, whose main function is to sup-

press protein aggregation (15), we next tested whether reducing endogenous levels of α B-crystallin in lens cells would influence inclusion body formation in 72Q mice. Mice homozygous for a gene disruption in the *Cryab* locus (16) were bred with 72Q mice, and lens sections from 72Q mice lacking α B-crystallin (*Cryab*^{-/-};72Q) were analyzed by confocal microscopy. The thickness of the shell of inclusion bodies in lens sections from *Cryab*^{-/-};72Q mice aged 3 weeks was nearly the same as that in *Cryab*^{+/+};72Q mice aged 12 weeks in some lens regions (compare Fig. 3, H and I with Fig. 3D). The shell thickness in *Cryab*^{-/-};72Q mice was also more irregular than in *Cryab*^{+/+};72Q mice, with more inclusions observed in younger fiber cells in the lens cortex (compare Fig. 3, H and I with Fig. 3B). These results demonstrate that α B-crystallin protects against 72Q inclusion body formation *in vivo* and suggest that regional variances exist in the expression level or functional capacity of α B-crystallin in the murine lens.

Expression of α -Synuclein in the Lens Results in Membrane and Cytoplasmic Localization—Next,

we analyzed cryostat sections of lenses from GFP (Fig. 5A), α -Syn-WT (Fig. 5K), and α -Syn-A53T mice (data not shown) by confocal microscopy. Dense GFP labeling was observed in all fiber cells, as predicted from previous characterization of the β B1-crystallin promoter (9). In lens sections from GFP mice analyzed at higher magnification, a diffuse GFP signal was observed on the epithelium (Fig. 5, B–D), a faint signal was observed on fiber cell membranes in the cortex (Fig. 5, E–G), and a prominent cytoplasmic localization was observed in the nuclear region (Fig. 5, H–J). The fluorescent signals from GFP expression in lens sections from α -Syn-WT (Fig. 5, K–T) and α -Syn-A53T mice (data not shown) were similar to that in mice expressing GFP alone. Unlike the 72Q mice, α -Syn-WT and α -Syn-A53T mice did not have large inclusion bodies. The mechanism for cataract formation in α -Syn-WT and α -Syn-A53T mice remains unclear. Since α -synuclein binds lipids and vesicles (17), we speculate that cataracts in these mice arise from an impairment of the structure and function of fiber cell membranes in the lens nucleus.

Expression of a Mutant *htt* Fragment in the Lens Results in Protein Aggregation—Laser light scattering has been used to noninvasively quantify protein aggregation leading to opacification over time in living mouse and human lenses (18). We

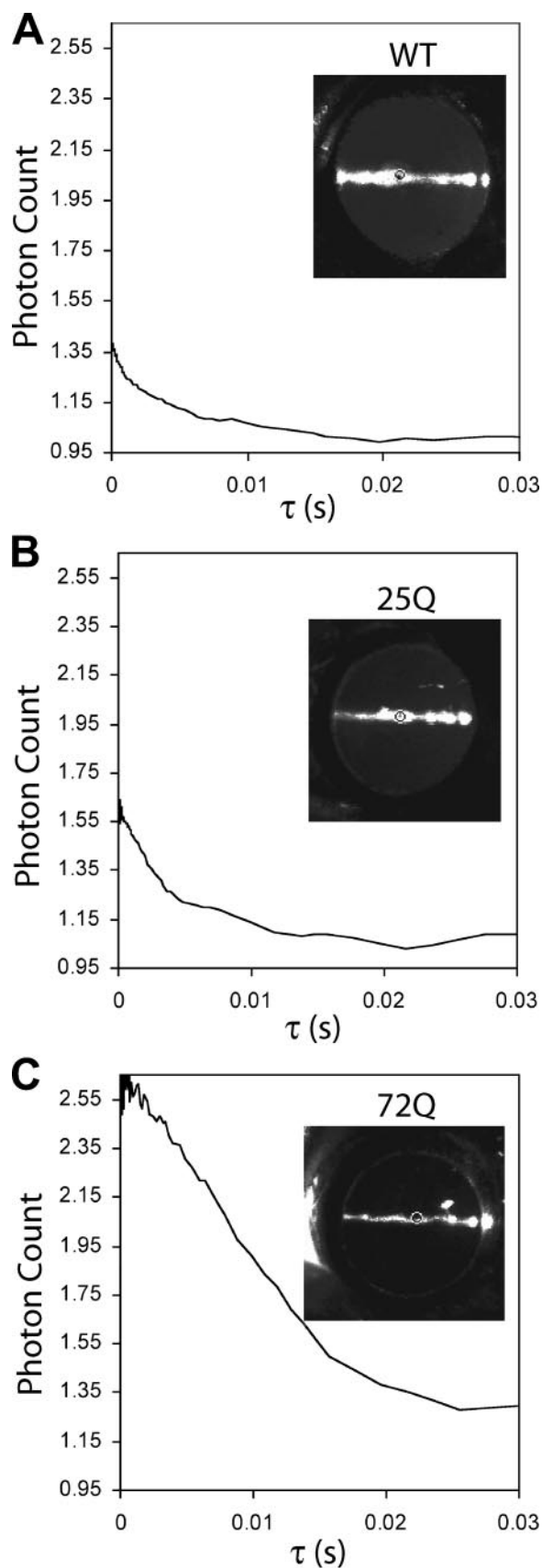


FIGURE 6. Targeted expression of a mutant htt fragment to the lens results in protein aggregation as detected by laser light scattering. A–C, representative autocorrelation function from the lens of WT (A), 25Q (B), or

used QLS to measure autocorrelation functions of the intensity fluctuations of light scattered from the supranuclear region, where opacities were observed to form first in slit-lamp views, from aged transgenic and control mice (Fig. 6). The QLS measurements suggested that the protein aggregates in the 72Q mice were larger than those that formed in the 25Q or WT mice. The QLS analysis (Fig. 6) was consistent with immunoblots of lens protein lysates that indicated that protein aggregates form in lenses from 72Q mice but not in 25Q and WT mice (Fig. 2).

DISCUSSION

Expression of mutant htt fragments or α -synuclein in the murine lens results in protein aggregation and opacification that can be easily detected using a sensitive, noninvasive slit-lamp examination. The lens-specific models of disease-relevant protein aggregation described here have several advantages over conventional animal models of protein misfolding diseases that make them attractive for preliminary screens of drug bioavailability, pharmacokinetics, and efficacy. The first major advantage is the rapid pathological outcome. Protein aggregation/cataract formation is detectable by 3 weeks of age in 72Q/ α -Syn-WT/ α -Syn-A53T mice and increases >15-fold by 8 weeks of age. In contrast, aggregate deposition in the brains of current animal models of HD or PD does not occur until \sim 2–15 months and progresses slowly (19). Thus, the effects of compounds on protein aggregation in our lens-specific models can be evaluated in trials that last as short as 2 weeks.

The second advantage is that disease-relevant protein aggregation can be evaluated in live animals without anesthesia using a slit-lamp biomicroscope and QLS. The lens models therefore provide a disease-relevant biomarker that can be evaluated rapidly and repetitively in a highly sensitive, noninvasive manner, unlike the slow, labor-intensive process of analyzing postmortem brain tissue.

The third advantage is that the lens-specific models may predict successful transport across the blood-brain barrier, an obstacle for potential therapeutic drugs for HD and PD. The ocular lens is neither vascularized nor innervated, and studies of drug permeability across the blood-lens barrier may identify drugs that are likely to cross the blood-brain barrier. Small compounds administered by various routes (oral, intravenous, intraperitoneal, intramuscular, or by eye drops) can permeate the blood-lens barrier and inhibit cataracts (20, 21). Although the lens-specific models will not be useful for studies of neuronal dysfunction or motor/behavioral/cognitive abnormalities relating to HD or PD, they should nonetheless be powerful tools to rapidly screen and identify compounds or genetic modifiers of disease-relevant protein aggregation that may prove effica-

72Q (C) mice aged 3–5 months. The rapid decay of the autocorrelation function in the lens of the WT mouse is characteristic of small mobile scatterers in a normal transparent lens (A). In the lens of the 25Q mouse, there is a noticeable change in the decay of the autocorrelation function, which is consistent with the initiation of aggregation (B). The dramatic change in the decay of the autocorrelation function in the 72Q mouse is a measure of large scatterers at the beginning cellular opacification (C).

Aggregation of Mutant Huntingtin and α -Synuclein in the Lens

cious in more physiologically relevant animal models of HD and PD.

Acknowledgments—We thank Anna Chepilinsky and Melinda Duncan for plasmids containing the α A- and β B1-crystallin promoters, respectively.

REFERENCES

1. The Huntington's Disease Collaborative Research Group (1993) *Cell* **72**, 971–983
2. DiFiglia, M., Sapp, E., Chase, K. O., Davies, S. W., Bates, G. P., Vonsattel, J. P., and Aronin, N. (1997) *Science* **277**, 1990–1993
3. Goedert, M. (2001) *Nat. Rev. Neurosci.* **2**, 492–501
4. Kruger, R. (2004) *J. Neurol.* **251**, Suppl. 6, VI/2–6
5. Dobson, C. M. (2003) *Nature* **426**, 884–890
6. Taylor, J. P., Hardy, J., and Fischbeck, K. H. (2002) *Science* **296**, 1991–1995
7. Kazantsev, A., Preisinger, E., Dranovsky, A., Goldgaber, D., and Housman, D. (1999) *Proc. Natl. Acad. Sci. U. S. A.* **96**, 11404–11409
8. Mahon, K. A., Chepilinsky, A. B., Khillan, J. S., Overbeek, P. A., Piatigorsky, J., and Westphal, H. (1987) *Science* **235**, 1622–1628
9. Taube, J. R., Gao, C. Y., Ueda, Y., Zelenka, P. S., David, L. L., and Duncan, M. K. (2002) *Transgenic Res.* **11**, 397–410
10. Outeiro, T. F., and Lindquist, S. (2003) *Science* **302**, 1772–1775
11. Seeberger, T. M., Matsumoto, Y., Alizadeh, A., Fitzgerald, P. G., and Clark, J. I. (2004) *J. Biomed. Opt.* **9**, 116–120
12. Goldstein, L. E., Muffat, J. A., Cherny, R. A., Moir, R. D., Ericsson, M. H., Huang, X., Mavros, C., Coccia, J. A., Faget, K. Y., Fitch, K. A., Masters, C. L., Tanzi, R. E., Chylack, L. T., Jr., and Bush, A. I. (2003) *Lancet* **361**, 1258–1265
13. Scherzinger, E., Lurz, R., Turmaine, M., Mangiarini, L., Hollenbach, B., Hasenbank, R., Bates, G. P., Davies, S. W., Lehrach, H., and Wanker, E. E. (1997) *Cell* **90**, 549–558
14. Burke, J. R., Enghild, J. J., Martin, M. E., Jou, Y. S., Myers, R. M., Roses, A. D., Vance, J. M., and Strittmatter, W. J. (1996) *Nat. Med.* **2**, 347–350
15. Clark, J. I., and Muchowski, P. J. (2000) *Curr. Opin. Struct. Biol.* **10**, 52–59
16. Brady, J. P., Garland, D. L., Green, D. E., Tamm, E. R., Giblin, F. J., and Wawrousek, E. F. (2001) *Investig. Ophthalmol. Vis. Sci.* **42**, 2924–2934
17. Rochet, J. C., Outeiro, T. F., Conway, K. A., Ding, T. T., Volles, M. J., Lashuel, H. A., Bieganski, R. M., Lindquist, S. L., and Lansbury, P. T. (2004) *J. Mol. Neurosci.* **23**, 23–34
18. Ansari, R. R., King, J. F., Seeberger, T., and Clark, J. I. (2003) *Proc. SPIE* **4951** (Ophthalmic Technology XIII), 168–176
19. Levine, M. S., Cepeda, C., Hickey, M. A., Fleming, S. M., and Chesselet, M. F. (2004) *Trends Neurosci.* **27**, 691–697
20. Hiraoka, T., Clark, J. I., Li, X. Y., and Thurston, G. M. (1996) *Exp. Eye Res.* **62**, 11–19
21. Hiraoka, T., and Clark, J. I. (1995) *Investig. Ophthalmol. Vis. Sci.* **36**, 2550–2555